

We are IntechOpen, the world's leading publisher of Open Access books Built by scientists, for scientists

6,900

Open access books available

185,000

International authors and editors

200M

Downloads

Our authors are among the

154

Countries delivered to

TOP 1%

most cited scientists

12.2%

Contributors from top 500 universities



WEB OF SCIENCE™

Selection of our books indexed in the Book Citation Index
in Web of Science™ Core Collection (BKCI)

Interested in publishing with us?
Contact book.department@intechopen.com

Numbers displayed above are based on latest data collected.
For more information visit www.intechopen.com



Shot Peening of Austempered Ductile Iron

Ann Zammit

Additional information is available at the end of the chapter

<http://dx.doi.org/10.5772/intechopen.79316>

Abstract

Austempered ductile iron (ADI) is a type of heat-treated cast iron, which offers numerous positive advantages including: good combination of mechanical properties and damping characteristics, lower density than steel and the possibility of casting components into near-net shape. However, surface engineering techniques are necessary to extend the use and prolong the lifetime of ADI engineering components. One such treatment for improving the bending fatigue strength of ADI is shot peening. This treatment creates compressive residual stresses and high dislocation densities at the surface of the treated components. However, the shot peening process is not always beneficial in improving the tribological characteristics of ADI. Its behaviour depends on the type of wear mechanism, applied loads, lubrication, heat treatment process parameters and the resulting surface finish of the components. This chapter will look into the effect of shot peening on ADI in more detail and will delve into a case study, which was carried out to analyse the bending fatigue resistance and tribological characteristics of Cu-Ni-alloyed ADI.

Keywords: cast iron, austempered ductile iron, graphite nodules, upper ausferrite, shot peening, bending fatigue, tribology, surface engineering

1. Introduction

Compared to other ferrous materials, austempered ductile iron (ADI) has marked economic advantages such as low melting temperature, low shrinkage, excellent castability, good machinability and high damping capacity. Its versatility and wide range of properties make it widely used in the transportation industries, defence, heavy machinery, agricultural machinery and for general engineering applications. ADI can compete with steel on considerations of strength, for a given level of ductility. However, some alloyed and hardened steels exhibit better properties than ADI, and the use of ADI is limited when extreme tensile strength is

required. As a raw material, ADI is cheaper than steel. It also has a lower manufacturing cost due to the possibility of casting the components to near-net shape. The cost and weight of ADI per unit of yield strength can compete with cast and forged aluminium, and forged steel. ADI exhibits higher damping characteristics than steel, leading to lower noise emission and less vibrations. The presence of graphite in ADI dampens vibrations 40% faster than in steel gears, and it also results in a 10% reduction in density compared to steel.

ADI is a type of cast iron, more commonly referred to as ductile iron, having an austempering heat treatment process applied to it. It is made up of graphite nodules in a matrix of acicular ferrite and retained austenite frequently referred to as ausferrite (**Figure 1**). Optimum properties are obtained when the chemical alloy composition, solidification micro-structure and heat treatment parameters are carefully controlled. The austempering heat treatment cycle (**Figure 2**) consists of first austenitising the ductile iron to temperatures between 850 and 1000°C, followed by quenching in a salt or oil bath. The bath is maintained between 230 and 450°C, a temperature above the martensite start temperature M_s and left there for sufficient time to transform the austenite to ausferrite. This is followed by cooling to room temperature.

The mechanical properties of ADI depend on the parameters of the austempering process, which determine the morphology of the ferrite, the volume fraction of retained austenite, the carbon content in the retained austenite, and the presence or absence of martensite and iron carbides in the austenite or ferrite. In general, the tensile strength of ADI varies from around 1500 MPa with a corresponding 1% elongation, to lower tensile strengths (900–1200 MPa) and higher corresponding elongations of up to 12%. The former group of ADIs is produced at lower austempering temperatures of 230–330°C and exhibits high hardness (~50–54 HRC), but limited ductility. These are used for applications requiring high resistance to contact stress. ADIs having lower tensile strength, which are produced at higher austempering temperatures of 350–400°C, have lower hardness ranging from around 23 to 34 HRC, but have high toughness and ductility [3]. This range of ADIs consist of structures with greater amounts of

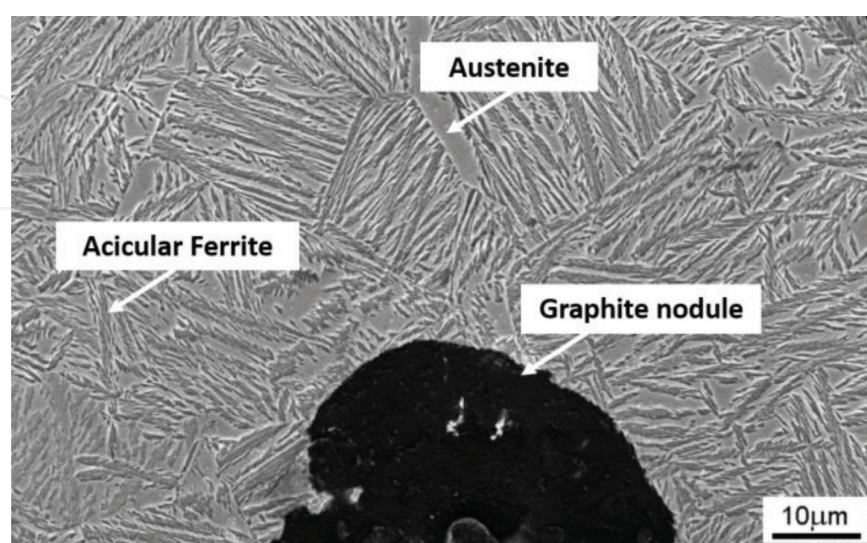


Figure 1. Typical micro-structure of ADI (austenitised at 900°C for 2 hours, austempered at 360°C for 1 hour) [1].

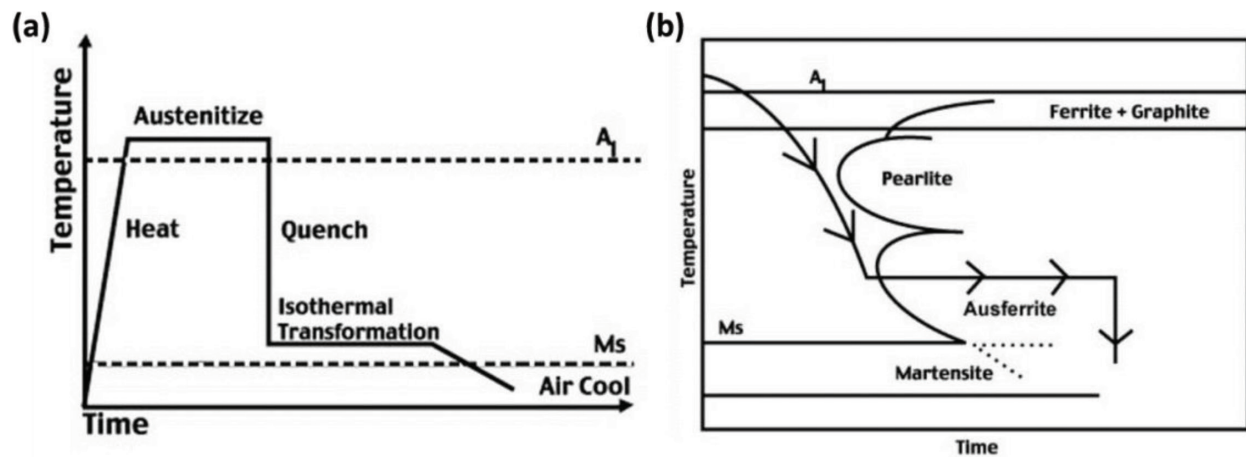


Figure 2. (a) Temperature-time plot for a typical austempering treatment and (b) austempering treatment superimposed on an isothermal transformation diagram [2].

austenite (V_γ), having high carbon content (C_γ) and provide a bending fatigue strength in the region between 200 and 500 MPa as reported in various studies carried out on both alloyed and unalloyed ADI [4–8].

When ADI engineering components require high toughness and ductility at the core of the component coupled with high bending fatigue strength and good tribological characteristics at the surface, the ADI can be first austempered in the higher temperature range of 350–400°C to obtain upper ausferrite. It is subsequently engineered to improve the surface properties and obtain the fatigue and tribological characteristics required by the intended application, using processes such as shot peening.

2. Shot peening

Shot peening (SP) is a conventional mechanical surface treatment during which the surface of a material is bombarded by spherical media (called *shot*) arriving at high velocity and under controlled conditions. During SP, shots are accelerated towards the surface using air pressure and a nozzle or a centrifugal wheel. Shots impart forces that form a dimple by plastic deformation and radial stretching of the material. The numerous dimples on the surface create several of such plastically deformed hemispheres, while the elastically stressed region tries to recover to the fully unloaded state. These inhomogeneous elastic-plastic deformations induce high residual compressive stress and high dislocation densities in the surface and to a depth of circa 120–500 μm [9]. Their magnitude is a function of the mechanical properties of the target material and is at least equal to half the yield strength of the material being peened [10].

The essential parameters of the SP process can be classified into three groups: shot (shape, hardness and size), workpiece (hardness, chemical composition, crystal structure, geometry) and flow parameters (shot velocity, impact angle, mass flow rate, peening time, coverage). These parameters need to be carefully controlled in order to achieve a uniform distribution of compressive stresses on the surface of a component.

The induced compressive layer and work hardening increase the resistance to crack initiation and propagation, which in turn prolongs components' lifetime. In fact, SP has been used for years to extend the bending fatigue life of various engineering components in the transport industry, mainly for automobile and aircraft parts. Such components include gears, axles, springs, connecting rods, crankshafts, I-beams in heavy duty applications, compressors, turbine rotors and shafts. SP can be applied to the whole component, or just confined to parts of the component that are expected to be highly stressed. For example, in gears, one can SP the entire gear tooth or alternatively focus the SP only at the tooth root fillets, which are exposed to the highest stress.

Although SP is not a new process, it is still very popular and has evolved considerably in the late twentieth and early twenty-first centuries. A great deal of research has been carried out to study the effects of SP on the materials being treated, including metallurgical, mechanical, and geometrical effects and also the effects of SP on the mechanical properties, tribological characteristics and corrosion resistance of a wide range of metals and alloys [11]. Recently, advanced surface modification technologies show the use of variants of the traditional SP process, four of which are shown in this issue, namely ultrasonic SP, severe SP (SSP), surface mechanical attrition treatment (SMAT) and duplex SP. Other variants of SP can be found in literature, including laser shock peening (LSP), micro-peening, cavitation shotless peening and ball or roller burnishing.

3. Shot peening of ADI

The high strains applied by the high-pressure impact of the shots on the surface of ADI are higher than the yield strength of the material, and both the ferrite and the austenite undergo plastic deformation. The ferrite work hardens with an increase in the dislocation density, while the austenite has the ability to cold work and to locally transform into martensite at high plastic deformation. The transformation induced plasticity (TRIP) phenomenon has been studied by various researchers [12, 13] and shown to depend on the carbon content in the austenite, its size and morphology and distribution within the structure.

As a result of work hardening and phase transformation, the hardness at the surface following SP of ADI increases by approximately 40–60% [11, 14–19]. Apart from an increase in the surface hardness, SP also results in the creation of compressive residual stresses of around 700–1000 MPa [15–19]. The residual compressive stresses caused by SP increase the dislocation density hindering dislocation motion. The stress-induced austenite to martensite transformation also results in volume expansion further creating local compressive stresses.

3.1. Influence of shot peening on bending fatigue strength of ADI

Shot peening is known to improve the bending fatigue properties of ADI [14, 15, 20, 21]. The improvement of bending fatigue resistance following SP is due to the formation of a compressed layer beneath the surface of the SP component. Cracks tend not to initiate or

propagate in surfaces upon which a compressive force is acting. The induced compressive stresses shift crack nucleation to the sub-surface and hinders fatigue crack propagation at the surface. Apart from hardening the surface, SP also eliminates microscopic defects, machining marks and grinding defects. This also increases the bending fatigue strength. However, Uematsu et al. [22] showed that SP cast iron containing spheroidal vanadium carbides (VCs), dispersed in a martensitic matrix, did not eliminate large casting voids. These voids and clusters of VCs served as sources of crack initiation, and hence SP did not improve the bending fatigue strength in this particular case.

3.2. Influence of shot peening on tribological characteristics of ADI

Wear of materials is a complex phenomenon, and depends on the running conditions and the properties of the tribopair materials. SP should be beneficial in reducing wear rates because of the high hardness due to work hardening, stress-induced austenite to martensite transformation, and residual compressive stresses at the surface [10, 23, 24]. Compressive stresses prevent micro-cracks from forming, thus inhibiting pitting or spalling. Kobayashi and Hasegawa [25] showed this to be true for carburised steel gears. This was attributed to the compressive stress suppressing cracking and delaying crack growth. Champaigne [10] and Townsend and Zaretsky [26] reported an improvement in the contact fatigue life of SP steel gears of around 1.5 times. In another study, Townsend [27] reported that a higher peening intensity (0.38–0.43 mmA) resulted in higher compressive stresses, and hence lead to a 10% rolling contact fatigue life (L_{10}) of 2.15 times that of the carburised gears peened with an intensity of 0.18–0.23 mmA. Adamović et al. [28] investigated the sliding wear characteristics of ground and SP steel under boundary lubrication, and reported a slight decrease in coefficient of friction and a 30% increase in the wear resistance after SP.

The effect of the rough SP surfaces on the tribological behaviour has been reported in a number of articles. The dimpled surface is sometimes considered to be favourable in lubricated contact, which acts as reservoirs that aid in the retention of the lubricant and maintaining a full film thickness between meshing teeth. Better lubrication reduces fretting, noise, spalling, scuffing and the operating temperature by reducing friction. That said, Vaxevanidis et al. [29] still reported improved sliding wear resistance of SP tool steel tested under dry conditions. A higher coefficient of friction was reported at the beginning of the test, but as the test progressed, this decreased to a lower value than that of specimens, which were not SP. This can be attributed to flattening of the rough surfaces during the wear test.

In contrast, studies by other researchers show no improvement in the tribological characteristics of surfaces after SP [30–32]. The reason given is that surface roughening counterbalances the positive effects of compressive stresses and hardening caused by SP.

Very few works have been conducted to study the tribological behaviour of SP ADI [30, 31]. Work by Sharma [31] showed that at a given load, the contact fatigue life of SP Mo-Ni ADI austempered at 230°C is 35–45% lower than that of carburised steel. The author attributed this to the rougher surface and a lower hardness of the SP ADI when compared to carburised steel. Lubricated rolling contact fatigue tests carried out by Ohba et al. [30] showed that SP Cu-alloyed ADI exhibited similar wear rates to corresponding as-austempered specimens.

This was attributed to surface roughening, which counterbalances the positive effects of compressive stresses and hardening caused by SP.

3.3. Case study: shot peening of Cu-Ni-alloyed ADI

This section is related to a study, which was conducted to address the inconsistencies related to the tribological characteristics of SP ADI. A Cu-Ni-alloyed ADI having the composition shown in **Table 1** was used for this study [16–19]. Ductile iron samples were first austenitised at a temperature of 900°C for 2 hours and subsequently austempered at 360°C for 1 hour. Following the austempering process, this material had an upper ausferrite matrix with an yield strength of 737 MPa, a tensile strength of 1012 MPa and an elongation of 7%. SP was done up to full coverage with S330 steel shots and with an Almen intensity of 0.38 mmA. The stand-off distance was 90 mm, while the angle of impingement was set at 90°. The surface roughness R_a following SP was measured to be 3.1 μm .

As indicated in Section 2, SP of austempered ductile iron results in strain-induced phase transformation from the face-centred cubic (FCC) austenite to body centred tetragonal (BCT) martensite. This can be observed in the X-ray diffraction pattern presented in **Figure 3**. The top pattern, which is for the SP specimen, does not show any of the austenite peaks present in the as-austempered ductile iron (bottom pattern in **Figure 3**), suggesting that only ferrite and martensite peaks are present and that the strain induced during SP has transformed the austenite to martensite. Similar findings are commonly reported in ferrous alloys having retained austenite present in the initial micro-structure before SP [14, 15, 23, 33].

The SP-induced work hardening and phase transformation result in an increase of the surface hardness of 43% from 370 to 535 HV (**Figure 4(a)**) and decreases steadily towards the interior of the specimen. This is in agreement with results reported in literature, where the typical hardness increase following SP of ADI is in the range of 40–60% [14, 15]. The depth of the SP layer was measured from the hardness-depth profile (**Figure 4(a)**) and is approximately 400 μm . The maximum compressive stress occurring at the SP surface has a value of 975 MPa (**Figure 4(b)**), which is 67% greater than the yield strength of the material. Similar values of compressive stress for the Cu-Mn ductile iron austempered at 380°C were reported by Ebenau et al. [15].

3.3.1. Bending fatigue resistance of shot-peened Cu-Ni ADI

As a result of SP, both the mean bending fatigue strength and the fatigue life of the Cu-Ni ADI were increased [18]. **Figure 5** shows the S-N curve for both the as-austempered and SP condition. It can be noted that the fatigue strength increased by approximately 60%, that is from 250 to 390 MPa. The improvement in fatigue life of around 35% was noted at all stress levels. On

Element	C	Si	Cu	Ni	Mn	P	Mg	Al	S	Fe
Wt.%	3.26	2.36	1.63	1.58	0.24	0.011	0.057	0.024	0.006	Bal.

Table 1. Chemical composition of the Cu-Ni-alloyed ductile iron.

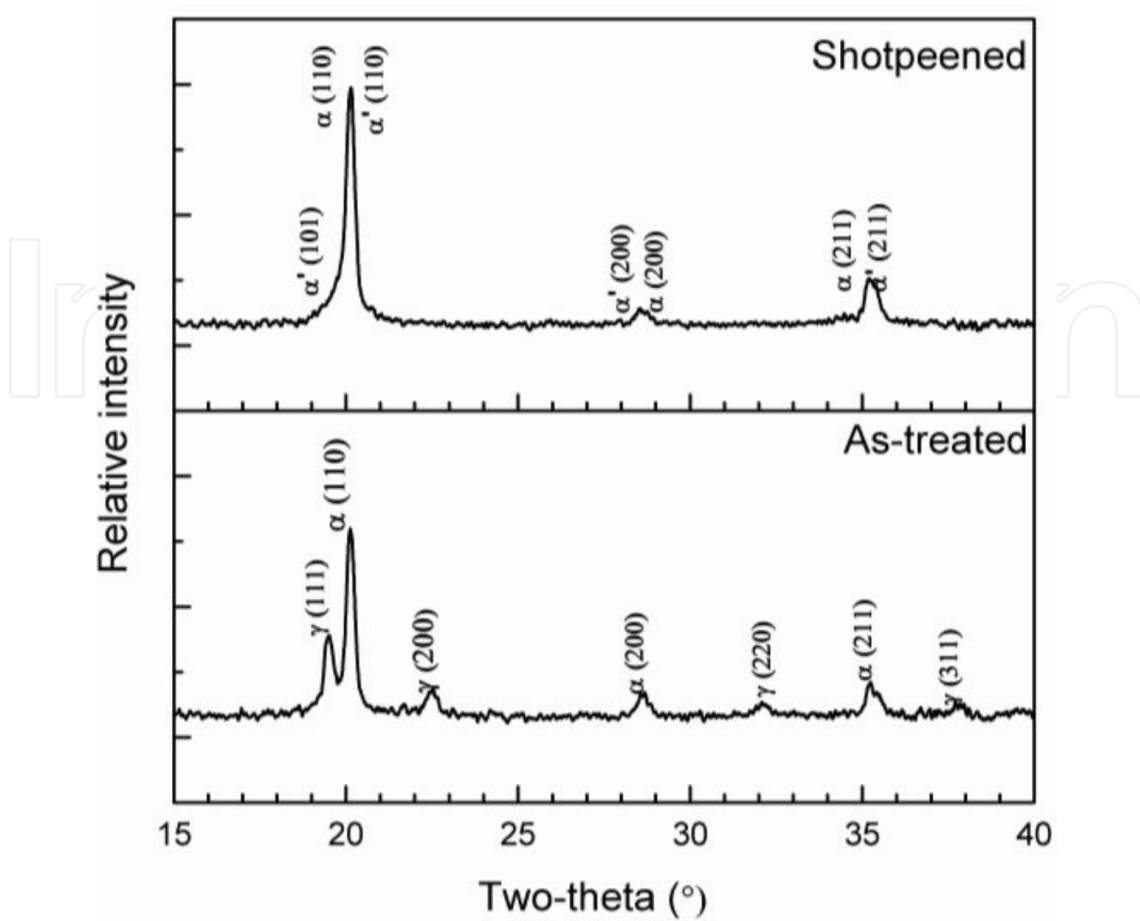


Figure 3. X-ray diffraction patterns of polished as-treated and shot-peened ADI (S330, intensity = 0.38 mmA) [18].

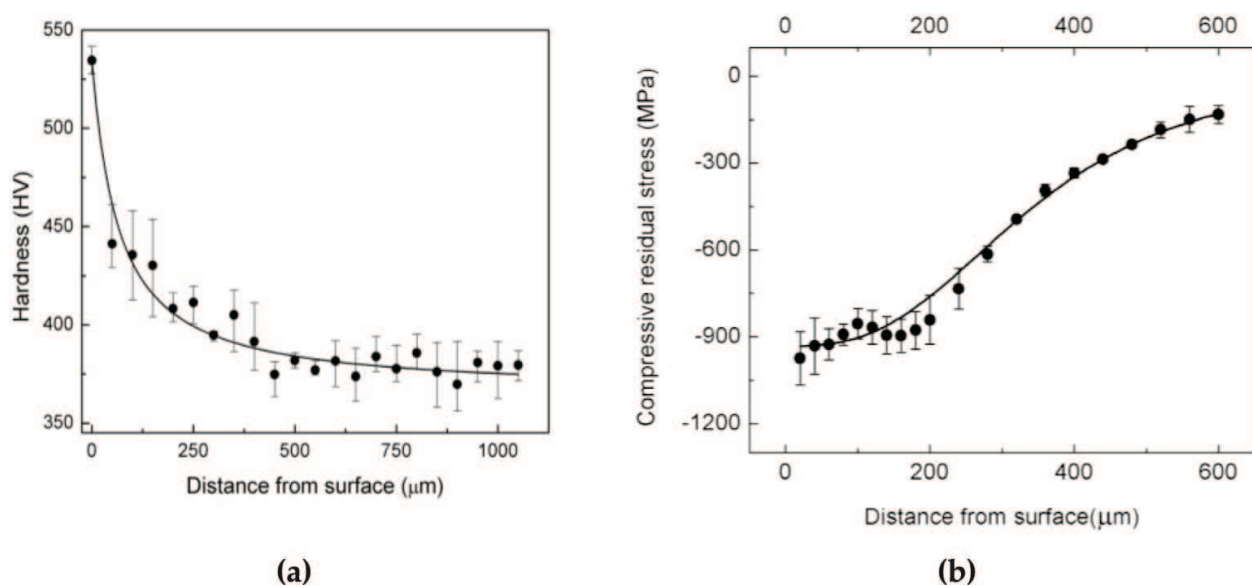


Figure 4. (a) Micro-hardness-depth profile of shot-peened ADI (S330, intensity = 0.38 mmA) and (b) residual stress-depth profile of shot-peened ADI (S330, intensity = 0.38 mmA) [18].

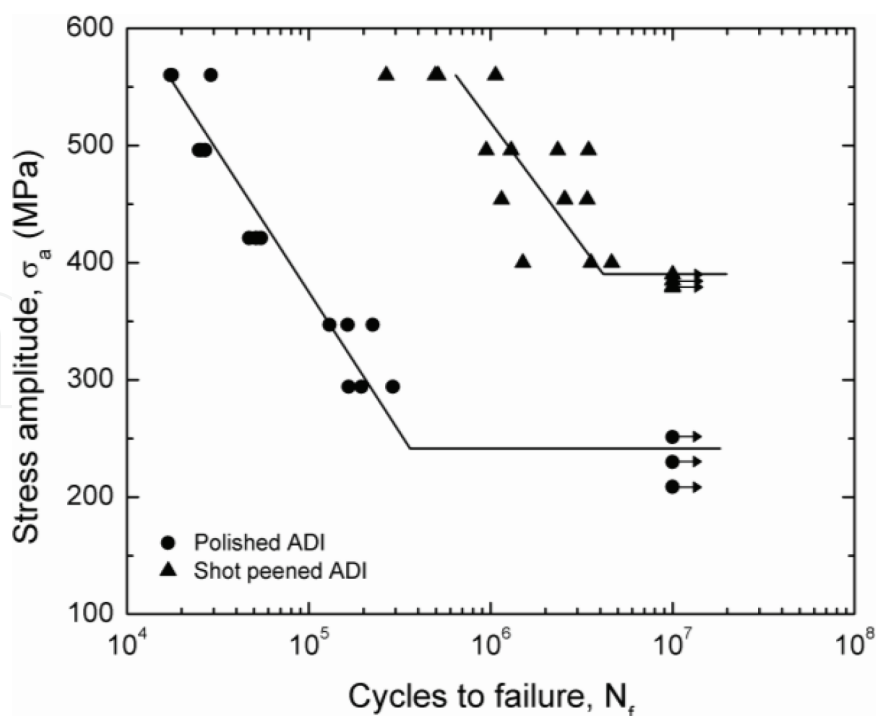


Figure 5. S-N curves for polished as-austempered ductile iron and SP ADI specimens [18].

the one hand, the results obtained for SP ADI (390 MPa) are similar to those obtained in other studies conducted by Mhaede et al. [34] and Ochi et al. [35] for unalloyed ADI, and by Benam et al. [14] for Cu-Ni-alloyed ADI. On the other hand, however, Ebenau et al. [15] reported values of 560 MPa when carrying out bending fatigue tests on SP Cu-Mn ADI austempered at 380°C. Surprisingly, these high values were obtained using the same S330 shots used in the present investigation: similar peening pressure of 3 bar and with recorded maximum residual compressive stress of 700 MPa. These results could potentially be explained in terms of differences in chemical compositions or heterogeneity in micro-structures.

The fatigue ratio, which is the ratio of the fatigue limit to the tensile strength, is 0.31 and 0.39 for the polished and SP specimens, respectively. This ratio is in agreement with British Cast Iron Research Association (BCIRA) reports that quote a fatigue ratio of 0.37 for austempered irons with tensile strengths in the range of 900–1000 N/mm² [36]. Johansson et al. [37] obtained higher endurance ratios of around 0.44, which were obtained in irons with tensile strengths in the range of 1000–1200 N/mm² produced by austempering between 350 and 375°C.

When comparing the bending fatigue strength obtained for the ADI in the present study to that for the carburised steel, it can be noted that the performance of carburised steel is far superior. Bending fatigue strengths of between 850 and 1500 MPa have been reported in a number of studies. This can be attributed to the harder surfaces (approximately 700 HV) and the deeper carburised layers (approximately 1.2 mm).

The crack propagation deflected along the graphite-matrix interface is shown in a cross section of a fractured specimen in **Figure 6**, which indicates a relatively weak interface between graphite nodules and the matrix. **Figure 7** also shows nodule debonding from one of the fractured

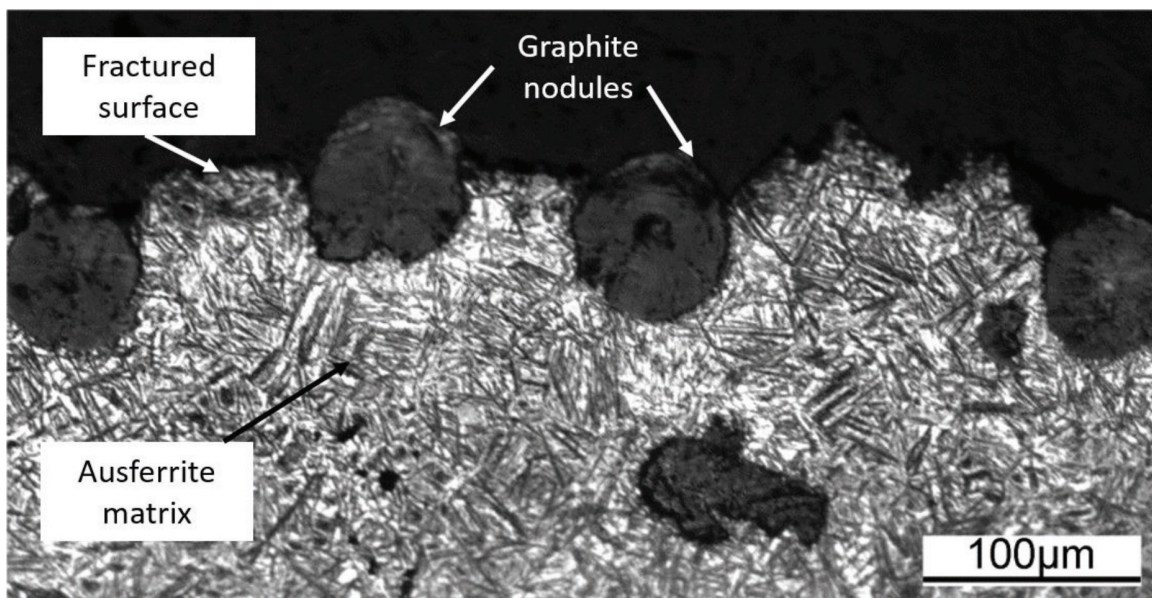


Figure 6. Crack propagation along graphite-matrix interface for a shot-peened ADI specimen [18].

surfaces. When traversing between graphite nodules, cracks were seen to pass through the lath of austenite and ferrite or through the austenite/ferrite interface, these being paths of least resistance. Similar results were also reported by Voigt [38] and Tayanç et al. [39]. Therefore, if nodules are sometimes considered as defects, the high toughness of stable austenite makes up for this negative effect. Crack propagation is also affected by the high toughness and ductility of the ausferritic micro-structure, making it a strong crack arrester. This structure absorbs the energy of the advancing crack during fracture, arresting the crack or deflecting it. In addition, ausferrite can strain harden during cyclic loading, providing high plastic deformation, which further hinders crack growth. Tanaka et al. [40] measured the hardness of upper ausferritic matrix after being subjected to different number of cycles during bending fatigue tests. The hardness of the matrix increased with longer number of cycles. Apart from strengthening by plastic deformation, unstable austenite can transform to martensite as the crack advances. The accompanying volume change, resulting in a compressed zone ahead of the crack tip, may retard crack growth, if not arrest it completely.

The extent to which the nodules can affect the fatigue behaviour of ADI depends on the nodularity where a high nodularity provides a better continuity of the matrix with less stress raisers. Furthermore, the nodule size, count and distribution are of equal importance. A high count, a smaller diameter and evenly distributed nodules decrease intercellular micro-segregation of elements. This results in an increase in the fracture toughness and fatigue resistance of ADI.

3.3.2. Dry sliding wear resistance of shot-peened Cu-Ni ADI

Dry sliding wear tests were carried out on the Cu-Ni ADI using a conventional pin-on-disk tribometer using two different applied pressures, 2.5 and 10 MPa [16]. **Figure 8** shows the wear factor K of the as-austempered DI and SP ADI specimens as a function of sliding distance. It can be noted that there is no difference between the wear rates for the two surface

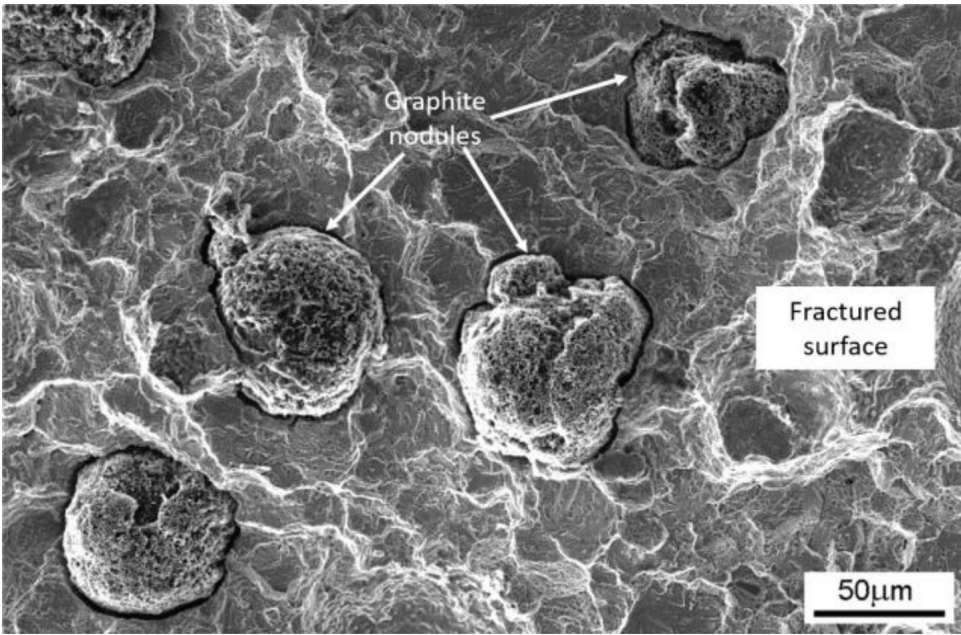


Figure 7. Graphite nodules attached to one of the fractured surfaces of an as-austempered DI specimen [18].

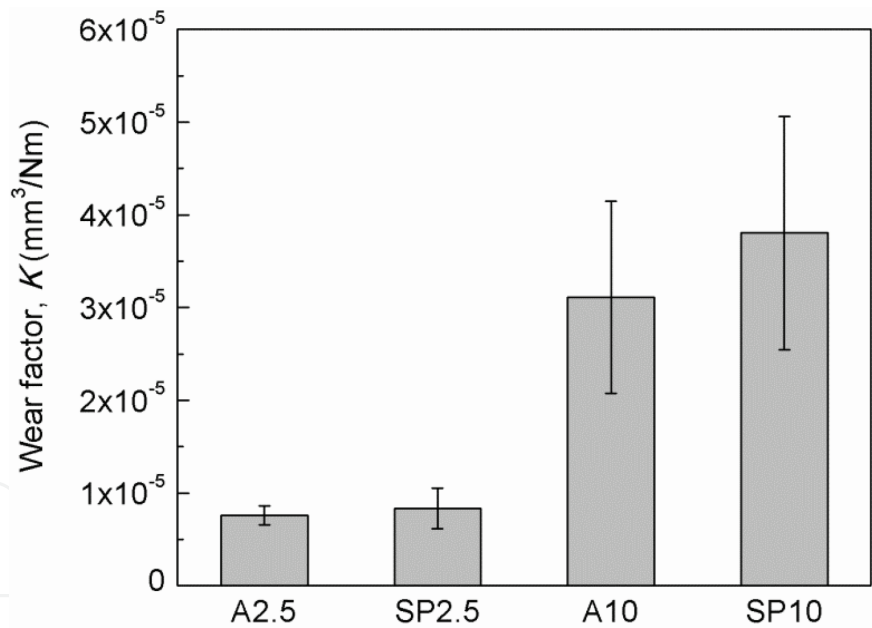


Figure 8. Wear factors of as-austempered ductile iron (A) and shot-peened ADI (SP) samples [16].

conditions: as-austempered DI and SP ADI specimens at the two applied loads. This indicates that SP did not result in an improvement in the dry sliding wear resistance. This suggests that a higher original hardness (535 HV for SP specimens compared to 370 HV for as-austempered specimens) does not necessarily result in better wear resistance. It may be argued, however, that the potential improvement resulting from an increase in hardness is being counterbalanced by the increased surface roughness caused by SP.

The micro-hardness-depth profiles taken on cross sections of the worn specimens are shown in **Figure 9(a)**, while **Figure 9(b)** compares the surface hardness at both applied pressures of specimens before and after the wear tests. At a low applied pressure of 2.5 MPa, the micro-hardness of the worn surface of as-austempered specimens was measured to be around 19% higher than that of the bulk. The thickness of this hardened layer is around 100 μm and is due to strain hardening of the ausferritic matrix at the surface region, which predominates over any frictional heating effect. As a result of this plastic deformation, the material is stronger and causes surface flow and the micro-structure to distort, as shown in **Figure 10(a)**.

It can be noted that the hardness of SP specimens decreases from 535 to 450 HV (**Figure 9**) after testing at the lower applied pressure of 2.5 MPa. This is probably due to the removal of part of the SP layer during the wear test, or tempering of the martensite, which was formed during the SP process.

On the other hand, the surface micro-hardness of specimens tested at the higher load is over 600 HV (**Figure 9**). This indicates a phase transformation to a high hardness phase. Micro-graphs show that a white non-etchable phase is present at the surface of the specimens tested with the higher load (**Figure 10(b)**). When the two surfaces slide over each other, most of the work done against friction is converted into heat, causing a general rise in temperature, as well as localised temperature spikes where an asperity makes contact with the mating surface. The resulting rise in temperature may modify the mechanical and metallurgical properties of the sliding surfaces, causing them to oxidise, or possibly melt. This high temperature transforms the ausferrite to austenite and can result in carbon diffusion from the nodules into the austenite and hence increasing the hardenability of the pin. Consequently, the critical cooling rate is lowered, resulting in the formation of untempered martensite at a slow cooling rate upon cooling of the pin and disk after the test is stopped. It is also possible that the austenite being produced due to the high temperatures reached at the asperities is rapidly cooled as heat is conducted into the underlying bulk material when the tip of the asperity breaks during sliding. As a result, the austenite transforms to martensite during testing.

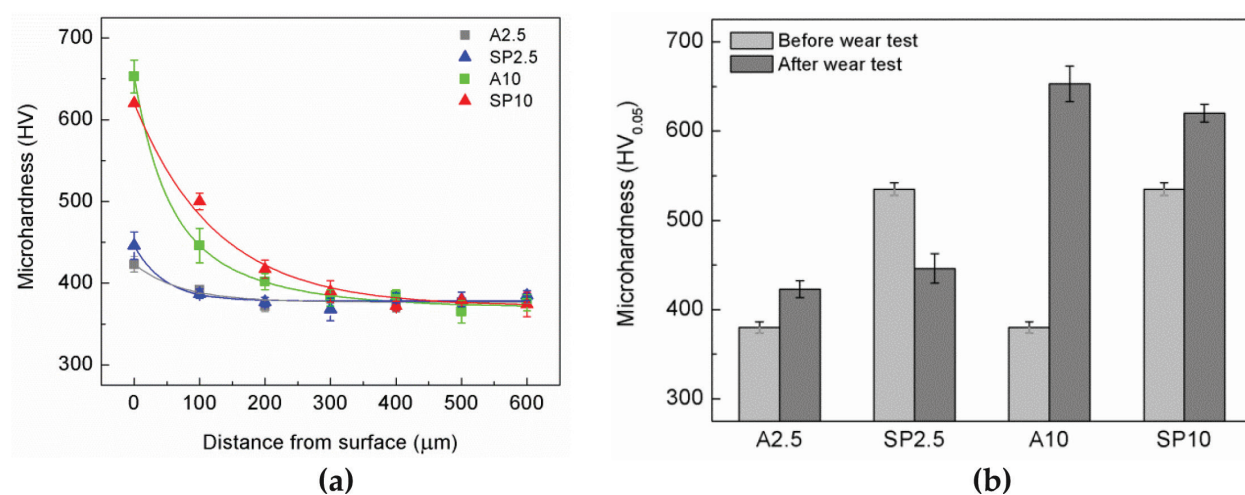


Figure 9. (a) Micro-hardness-depth profiles of cross sections of worn specimens and (b) surface hardness before and after dry sliding wear tests [16].

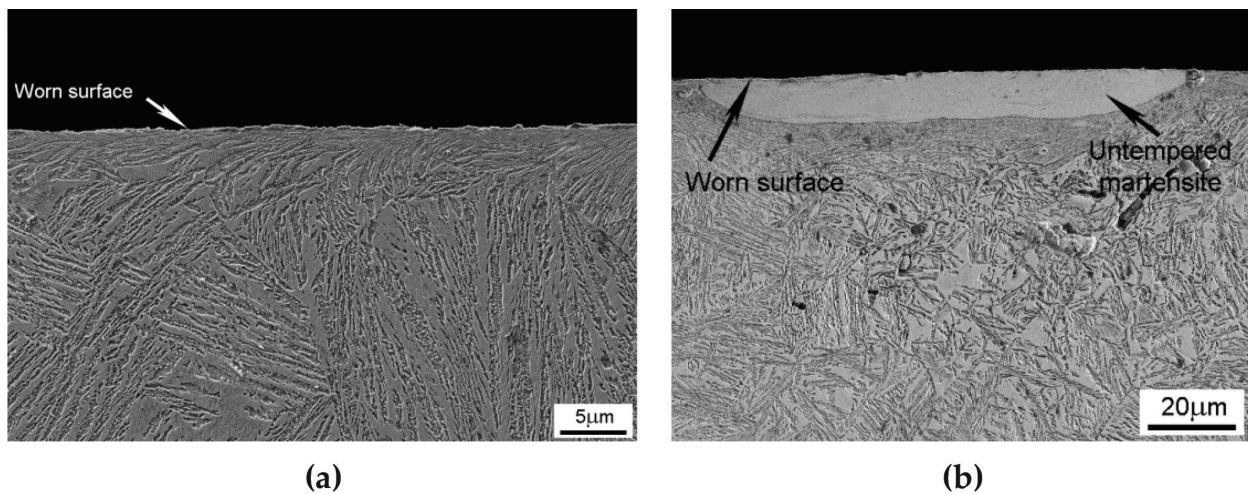


Figure 10. Micro-structure just below the worn surface of a specimen tested at an applied pressure of (a) 2.5 and (b) 10 MPa [16].

Fordyce et al. [41] also observed this white non-etchable layer during the unlubricated sliding wear of austempered spheroidal cast iron but not of as-cast spheroidal iron. Straffelini et al. [42] explained how the wear rate of ADI at high sliding speeds of 1.5–2.6 m/s was dominated by the formation and cracking of this white layer formed on the sliding surface. Sharma [31] has also shown that high loads applied during wear testing may transform the metastable austenite to martensite.

The presence of graphite nodules has a major influence on the wear rate of ADI as superficial graphite is smeared over the surface and aids in lubricating the surfaces in sliding contact. Graphite naturally has an inherent lubricating ability, being able to smear over the contacting surfaces. This lowers the friction coefficient and prevents metallic contact, hence reducing the adhesive bonding between the surfaces and material loss due to wear. Due to this, ADI components, for example railcar wheels, are sometimes run dry without the need of lubrication. Cracks have a tendency of passing through the graphite-matrix interface, this being the path of least resistance. On the other hand, a nodule may arrest crack propagation. Whether or not a crack is arrested or assisted to propagate as it reaches a graphite nodule would depend on the angle of approach. It follows that graphite nodules influence the propagation path.

3.3.3. Scuffing resistance of shot-peened Cu-Ni ADI

Figure 11(a) shows that during starved lubricated sliding wear tests, the SP Cu-Ni ADI (SP) specimens exhibited a higher scuffing wear resistance than corresponding as-austempered (A) specimens [43]. SP specimens survived 21×10^3 cycles, while the as-austempered specimens endured 2.3×10^3 cycles before failure. The improved scuffing performance due to SP might seem anomalous, since rough surfaces generally create low values of the specific film thickness λ and induce scuffing. However, the superposition of indentations arising from the SP process can be considered as an advantage in starved lubricated moving parts. These act as oil reservoirs by dragging the oil into them and generating a load-carrying hydrodynamic pressure. This decreases the pressure from the sliding surfaces, leading to longer lives for the

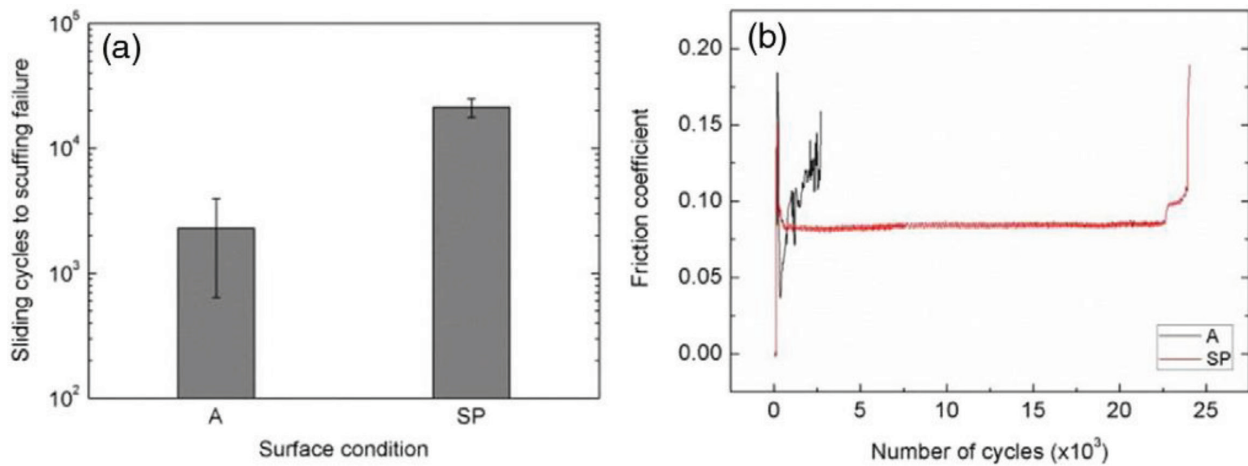


Figure 11. (a) Number of sliding cycles to scuffing failure for as-austempered (A) ADI and shot-peened (SP) ADI specimens and (b) friction coefficient evolution for lubricated sliding wear tests involving the as-austempered ADI and shot-peened ADI specimens [43].

SP specimens. On the other hand, the larger number of smaller asperities for the ground as-austempered specimens leads to a larger real area of contact upon application of the normal force and the presence of a very thin oil film. As a result, the number of sliding cycles to failure decreases due to plastic flow of the softer ADI specimens and micro-fracture of the asperities. This highlights the importance of the surface topography in asperity-asperity contact during sliding of components.

The higher scuffing resistance of the SP specimens could also be attributed to the high compressive stresses present in these specimens. It has been explained in previous sections that compressive stresses create a resistance to crack propagation and flaking of the surface. This was also attested by Adamović et al. [28], who reported a 30% improvement in the wear resistance of steels after SP.

Additionally, the SP specimens exhibit a lower value of coefficient friction at 0.08, when compared to that measured for their counterpart as-austempered specimens. This can be seen from the friction coefficient data of the lubricated sliding wear tests presented in **Figure 11(b)**. The coefficient of friction for the as-austempered specimens is seen to increase progressively as the test progresses. This is attributable to the larger number of small asperities of the as-austempered pin in contact with the disk. In contrast, the local traction at asperity contacts is reduced in the dimpled SP specimens, again as a result of the oil pockets on the surface. It is known that at lower levels of friction, the surface traction forces and sub-surface shear forces between two interacting bodies might not be sufficient to initiate crack growth and delamination. Hence, the lower friction for the SP specimens leads to longer number of cycles before the onset of failure. A lower coefficient of friction than that produced by ground surfaces was also reported for SP steel specimens [28] and for dented steel surfaces [44] under starved lubrication conditions.

The higher hardness of the SP specimens (~ 535 HV) should have also contributed to the improved scuffing resistance. The benefit of a high hardness in wear tests carried out under

starved lubrication conditions was also mentioned by Adamović et al. [28]. In fact, the hardness of mating surfaces is a crucial factor in avoiding scuffing.

It was also noted that the graphite nodules play a part in determining the scuffing resistance. In fact, as seen in **Figure 12** cracks emanate or stop at the nodules. This observation is similar to that mentioned earlier during bending fatigue [18] and dry sliding wear of ADI [16].

3.3.4. Rolling contact fatigue resistance of shot-peened Cu-Ni ADI

As-austempered and SP Cu-Ni ADI specimens were tested up to pitting failure using a cone-three ball tribosystem at an applied stress of 2.56 GPa [19]. **Figure 13** presents the Weibull probability plot for the tests, showing the percentage of specimens that will fail up to a specific number of cycles. The cumulative distribution function (CDF) is shown on the y-axis, while the number of rolling cycles to contact fatigue is shown on the x-axis. In this plot, the data points represent the number of cycles to failure of the ADI specimens.

Figure 13(b) shows the average contact fatigue lives for the as-austempered DI and SP specimens. Results show that the average contact fatigue life of SP specimens decreased by 72% when compared to the performance of the as-austempered specimens. Similarly, Sharma et al. [31] reported that SP lowered the contact fatigue life of ADI by 60%. Also, Vrbka et al. [46] report an 82% decrease in life of steel specimens following rolling contact fatigue tests. In the current study, austempering at 360°C resulted in a hardness of 370 HV, while SP increased the surface hardness to approximately 530 HV. Based only on hardness, one would expect an improvement in the contact fatigue resistance. Also, the residual compressive stresses present in SP layers (**Figure 4(b)**) should effectively reduce the maximum shear stress inside the Hertzian contact field, delaying crack nucleation and propagation.

However, the surfaces of the SP specimens have a higher surface roughness ($R_a = 3.1 \mu\text{m}$) than the counterpart as-austempered specimens ($R_a = 0.4 \mu\text{m}$). This leads to an extremely low

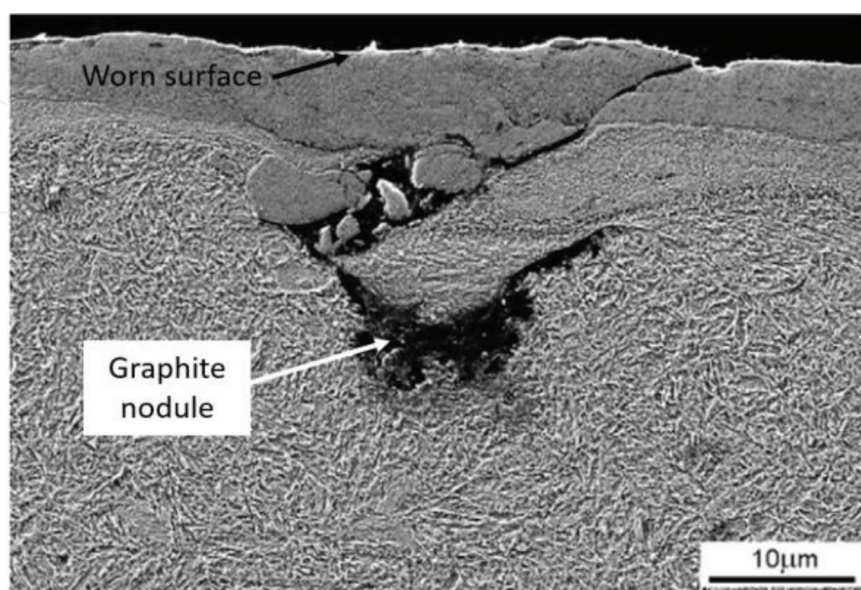


Figure 12. Micro-graph showing the influence of graphite nodules on crack initiation and/or propagation [43].

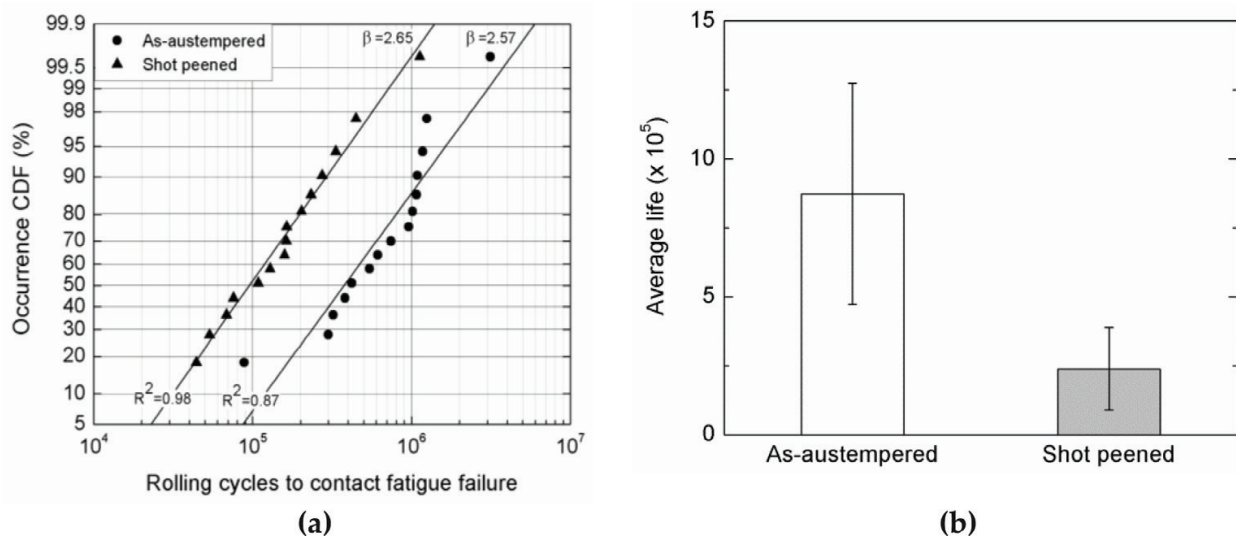


Figure 13. (a) Weibull probability plot for data obtained from rolling contact fatigue tests and (b) L10, L50, characteristic (η) fatigue lives for as-austempered and shot-peened ADI specimens [19, 45].

value of the specific film thickness λ of 0.05, which contrast with a corresponding value of 2.81 for the as-austempered specimens. A value of λ smaller than 0.4 denotes that a boundary lubricated condition exists, implying that peaks of the asperities of the SP specimens are penetrating the lubricant film. Contact, therefore, occurs between the asperities of the SP ADI cones and balls. Metal-to-metal contact is unavoidable and nearly all the load is supported by the asperities, defying the principal purpose of lubrication. Contact fatigue failure starts from the surface as a result of a presumably high coefficient of friction.

This might seem anomalous after having shown that under starved lubricated sliding wear, the dimples forming the rough surface of the SP specimens act as lubricant reservoirs, aiding in keeping the lubricant between the surfaces and serving to delay failure. One may have expected this positive attribute to apply also for the rolling tests. However, with the application of larger quantity of lubricant, smoother surfaces of the as-austempered samples proved to be more beneficial as it resulted in the formation of a full lubricating film. One should note that in contrast, all the specimens in the starved lubricated sliding wear tests were tested under boundary lubricated conditions. These results are in agreement with Zhai et al. [44] who report that the effect of surface dents is favourable under poorly lubricated conditions, but adverse under a well-lubricated environment. This means that the influence of dimpled surfaces on the tribological characteristics of the material depends on the lubrication regime.

For rough SP surfaces to operate in a fully lubricated condition, the minimum film thickness should be thicker than the combined surface roughness of the two interacting components. A thicker film is obtained by increasing the operating speed, the oil viscosity or the relative radius of curvature of the surfaces in contact. The elastic properties of the gear teeth and the applied load have relatively small influences on the lubricant film thickness. Increasing the load will only increase the elastic flattening (the width of the Hertzian contact band) and the contact area, without changing the geometry of the inlet region. Apart from the benefits of a thicker film, improving the performance of SP surfaces might be due to lower surface roughness. This can be achieved by either using shots having a smaller diameter, or by grinding/polishing the surface

after SP. In fact, rolling contact fatigue tests carried out by Ohba et al. [30] showed nearly equal fatigue lives for ground as-austempered DI and SP ADI using shots with a diameter of 0.1 mm. On the other hand, Vrbka et al. [46] report a deterioration in the rolling contact fatigue resistance of steel despite the use of shots having smaller diameters of 0.07 and 0.11 mm. One notes that shots used in the present study had diameters in the range of 0.85–1.2 mm. Results in this study [46] were improved when testing specimens, which were polished after SP, thus creating relatively smoother surfaces, in which the asperities did not protrude the lubricant film. However, grinding or polishing of SP surfaces might be challenging since extra care must be taken so as not to remove the SP layer and hence eliminate the beneficial effects, which result from SP (high hardness and compressive stresses at the surface).

4. Conclusion

The work presented in this chapter has hopefully contributed to a better understanding of the mechanical behaviour and tribological characteristics of both as-austempered ductile iron (ADI) and shot-peened (SP) ADI. A case study was presented in which bending fatigue tests and three different tribological tests were carried out on Cu-Ni-alloyed ADI. The major conclusions of can be summarised as follows:

1. After SP, a good balance between surface roughness, high surface hardness and hardened depth was obtained. Austenite transformed to martensite by the TRansformation Induced Plasticity (TRIP) phenomenon and the surface hardness increased by about 43% to a value of approximately 535 HV; the depth of the SP layer was approximately 400 μm , residual compressive stresses had a maximum value of 975 MPa and the surface roughness increased from 0.4 to 3.1 μm .
2. Rotating bending fatigue tests revealed that SP improved the bending fatigue strength of the Cu-Ni ADI by around 60% from 250 to 390 MPa. This was attributed to the induced compressive stresses that shift crack nucleation to the sub-surface and hinders fatigue crack propagation.
3. Dry lubricated sliding wear tests showed that SP did not result in an improvement in the dry sliding wear resistance of Cu-Ni ADI. The potential advantages resulting from the higher hardness at the surface, stress-induced austenite to martensite transformation and the residual compressive stresses of the SP specimens are counteracted by the induced surface roughness.
4. Starved lubricated sliding wear tests showed that SP resulted in an 800% improvement in the scuffing wear resistance of the ADI. The lower resistance to scuffing attested by the as-austempered specimens was attributed to plastic flow and micro-fracture of asperities. On the other hand, the superposition of indentations arising from the SP process acted as oil reservoirs and hence reduced surface traction forces. The higher scuffing resistance of the SP specimens was also partly attributed to the high hardness and high compressive stresses present in the surface of these specimens.

5. Lubricated rolling contact fatigue tests revealed that SP resulted in a 72% decrease in the average contact fatigue life when compared to the resulting fatigue life obtained by the as-austempered specimens. This was attributed to the rough surfaces of SP specimens, which in turn caused a low specific film thickness, leading to rolling in the boundary lubrication regime. In contrast, rolling of the polished as-austempered specimens was conducted in the presence of a full lubricant film, which is the ideal lubrication regime of components under rolling contact.

The SP process is constantly maturing, and many questions still remain open as the industry is continuously on the search for process improvements that improve and extend the service lifetime of components. For example, the improvement in surface roughness has improved the tribological characteristics, the ability to create textured nanostructured surface layers and also new equipment and techniques to characterise the treated surfaces [11].

Acknowledgements

The authors would like to acknowledge the positive impact of ERDF funding and the purchase of the testing equipment through the project: Developing an Interdisciplinary Material Testing and Rapid Prototyping R&D Facility (Ref. no. 012).

Author details

Ann Zammit

Address all correspondence to: ann.zammit@um.edu.mt

Department of Metallurgy and Materials Engineering, University of Malta, Msida, Malta

References

- [1] Zammit A. Tribological and mechanical characteristics of surface modified austempered ductile iron [PhD thesis]. University of Malta; 2014
- [2] Borui Casting International Ltd. Austempering Process for Ductile Iron [Internet]. Available from: <http://www.metals-china.com/austempering-process-for-ductile-iron-austempered-ductile-iron.html> [Accessed: 17-05-2018]
- [3] Harding RA. The production, properties and automotive applications of austempered ductile iron. *Kovove Materialy*. 2007;**45**:1-16
- [4] Shanmugam P, Rao PP, Udupa KR, Venkataraman N. Effect of microstructure on the fatigue strength of an austempered ductile iron. *Journal of Materials Science*. 1994;**29**:4933-4940. DOI: 10.1007/BF00356546

- [5] Bahmani M, Elliott R, Varahram N. The relationship between fatigue strength and microstructure in an austempered Cu–Ni–Mn–Mo alloyed ductile iron. *Journal of Materials Science*. 1997;**32**:5383–5388. DOI: 10.1023/A:1018631314765
- [6] Lin CK, Wei JY. High-cycle fatigue of austempered ductile irons in various-sized Y-block castings. *Materials Transactions (JIM)*. 1997;**38**:682–691. DOI: 10.2320/mater-trans1989.38.682
- [7] Lin CK, Hung TP. Influence of microstructure on the fatigue properties of austempered ductile irons—II. Low-cycle fatigue. *International Journal of Fatigue*. 1996;**18**:309–320. DOI: 10.1016/0142-1123(95)00108-5
- [8] Benam AS. Effect of shot peening on the high-cycle fatigue behavior of high-strength cast iron with nodular graphite. *Metal Science and Heat Treatment*. 2017;**58**:568–571. DOI: 10.1007/s11041-017-0056-6
- [9] Schulze V. Characteristics of surface layers produced by shot peening. In: *Proceedings of the 8th International Conference on Shot Peening*; 2002; Garmisch-Partenkirchen, Germany. 2002. p. 145
- [10] Champaigne J. Shot peening overview. Metal Improvement Company. 2001
- [11] Zammit A. Editorial: Special issue on shot peening. *Surface Engineering*. 2017;**33**:649–650. DOI: 10.1080/02670844.2017.1338552
- [12] Myszka D. Austenite-martensite transformation in austempered ductile iron. *Archives of Metallurgy and Materials*. 2007;**52**:475–480
- [13] Daber S, Rao PP. Formation of strain-induced martensite in austempered ductile iron. *Journal of Materials Science*. 2008;**43**:357–367. DOI: 10.1007/s10853-007-2258-6
- [14] Benam AS, Yazdani S, Avishan B. Effect of shot peening process on fatigue behavior of an alloyed austempered ductile iron. *China Foundry*. 2011;**8**:325–330
- [15] Ebenau A, Lohe D, Vohringer O, Macherauch E. Influence of shot peening on the microstructure and the bending fatigue strength of bainitic-austenitic nodular cast iron. In: *Proceedings of the ICSP-4*; Tokyo, Japan. 1990. pp. 389–398
- [16] Zammit A, Abela S, Wagner L, Mhaede M, Grech M. Tribological behavior of shot peened Cu–Ni austempered ductile iron. *Wear*. 2013;**302**:829–836. DOI: 10.1016/j.wear.2012.12.027
- [17] Zammit A, Hopkins L, Betts JC, Grech M. Austenite transformation in austempered ductile iron. In: *Materials Science and Engineering (MSE 2008)*; Nuremberg, Germany. 2008
- [18] Zammit A, Mhaede M, Grech M, Abela S, Wagner L. Influence of shot peening on the fatigue life of Cu–Ni austempered ductile iron. *Materials Science and Engineering: A*. 2012;**545**:78–85. DOI: 10.1016/j.msea.2012.02.092
- [19] Zammit A, Abela S, Michalczewski R, Wagner L, Mhaede M, Wan R, Grech M. Influence of shot peening on the rolling contact fatigue resistance of Cu–Ni austempered ductile iron. In: *Proceedings of the ICSP-12*; Goslar, Germany. 2014. pp. 38–73

- [20] Ezoe S, Hashimoto M, Asano I, Tanno Y. Effects of shot peening and heat treatment on endurance limits of austempered ductile cast iron gears. In: Proceedings of the ICSP-6; San Francisco, California, USA. 1996. pp. 14-23
- [21] Johansson M. Austenitic-bainitic ductile iron. Transactions of the American Fisheries Society. 1977;**85**:117-122
- [22] Uematsu Y, Kakiuchi T, Tokaji K, Nishigaki K, Ogasawara M. Effects of shot peening on fatigue behavior in high speed steel and cast iron with spheroidal vanadium carbides dispersed within martensitic-matrix microstructure. Materials Science and Engineering: A. 2013;**561**:386-393. DOI: 10.1016/j.msea.2012.10.045
- [23] Kirk D. Residual stresses and retained austenite in shot peened steels. In: Proceedings of the ICSP-1; Paris, France. 2013. pp. 271-278
- [24] Blackmore PA, Harding RA. The effects of metallurgical process variables on the properties of ADI. Journal of Heat Treating. 1984;**3**:310-325
- [25] Kobayashi M, Hasegawa K. Effect of shot peening on the pitting fatigue strength of carburised gears. In: Proceedings of the ICSP-4; Tokyo, Japan. 1990. pp. 465-476
- [26] Townsend DP, Zaretsky EV. Effect of shot peening on surface fatigue life of carburized and hardened AISI 9310 spur gears. NASA Technical Paper, 2047. 1982. pp. 5-12
- [27] Townsend DP. Improvement in surface fatigue life of hardened gears by high-intensity shot peening. NASA Tech Report 91-C-042. 1992
- [28] Adamovic D, Babic M, Jeremic B. Shot peening influence on tribological characteristics of surfaces. In: ICSP-7; Warsaw, Poland. 1999. pp. 350-358
- [29] Vaxevanidis NM, Manolakos DE, Koutsomichalis A, Petropoulos G, Panagotas A, Sideris I, Mourlas A, Antoniou SS. The effect of shot peening on surface integrity and tribological behaviour of tool steels. In: AITC-AIT; Parma, Italy. 2006
- [30] Ohba H, Matsuyama S, Yamamoto T. Effect of shot peening treatment on rolling contact fatigue properties of austempered ductile iron. Tribology Transactions. 2002;**45**:576-582
- [31] Sharma VK. Roller contact fatigue study of austempered ductile iron. Journal of Heat Treating. 1984;**3**:326-334
- [32] Peyrac C, Flavenot J. Optimisation of carburising and shot peening, in order to improve both bending and contact fatigue behaviour for gear applications. In: Proceedings of the ICSP-9; Paris, France. 2005
- [33] Watanabe Y, Hasegawa N, Namiki K, Hatano A. The influence of broken shots on peening effect of hard shot peening. In: Proceedings of the ICSP-4; Tokyo, Japan. 1990
- [34] Mhaede MH, Ibrahim KM, Wollmann M, Wagner L. Enhancing fatigue performance of ductile Iron by austempering and mechanical surface treatments. In: Proceedings of Arabcast. 2008

- [35] Ochi Y, Masaki K, Matsumura T, Sekino T. Effect of shot-peening treatment on high cycle fatigue property of ductile cast iron. *International Journal of Fatigue*. 2001;**23**:441-448. DOI: 10.1016/S0142-1123(00)00110-9
- [36] Gilbert GNJ. *An introduction to the Mechanical Properties of Nodular (SG) Cast Irons*. Alvechurch, Birmingham: BCIRA; 1986
- [37] Johansson M, Vesanen A, Rettig H. Austenitic-bainitic cast iron with spheroidal graphite as construction material for gears. *Antriebstechnik (BCIRA Translation T1507)*. 1976;**15**:593-600
- [38] Voigt RC. Microstructural analysis of austempered ductile cast iron using the scanning electron microscope. *Transactions of the American Fisheries Society*. 1983;**83-89**:253-262
- [39] Tayanc M, Aztekin K, Bayram A. The effect of matrix structure on the fatigue behaviour of austempered ductile iron. *Materials and Design*. 2007;**28**:797-803
- [40] Tanaka Y, Yang Z, Miyamoto K. Evaluation of fatigue limit of spheroidal graphite cast iron. *Materials Transactions (JIM)*. 1995;**36**:749-756
- [41] Fordyce EP, Allen C. The dry sliding wear behaviour of an austempered spheroidal cast iron. *Wear*. 1990;**135**:265-278. DOI: 10.1016/0043-1648(90)90030-E
- [42] Straffelini G, Pellizzari M, Maines L. Effect of sliding speed and contact pressure on the oxidative wear of austempered ductile iron. *Wear*. 2011;**270**:714-719. DOI: 10.1016/j.wear.2011.02.004
- [43] Zammit A, Abela S, Wagner L, Mhaede M, Wan R, Grech M. The effect of shot peening on the scuffing resistance of Cu-Ni austempered ductile iron. *Surface and Coatings Technology*. 2016;**308**:213-219. DOI: 10.1016/j.surfcoat.2016.06.089
- [44] Zhai X, Chang L, Hoeprich MR, Nixon HP. On mechanisms of fatigue life enhancement by surface dents in heavily loaded rolling line contacts. *Tribology Transactions*. 1997;**40**:708-714. DOI: 10.1080/10402009708983712
- [45] Zammit A, Abela S, Michalczewski R, Kalbarczyk M, Wagner L, Mhaede M, Wan R, Grech M. Rolling contact fatigue resistance of shot peened austempered ductile iron. *Tribologia*. 2014;**4**:137-147
- [46] Vrbka M, Křupka I, Svoboda P, Šperka P, Návrát T, Hartl M, Nohava J. Effect of shot peening on rolling contact fatigue and lubricant film thickness within mixed lubricated non-conformal rolling/sliding contacts. *Tribology International*. 2011;**44**:1726-1735. DOI: 10.1016/j.triboint.2011.06.019